

# NiMo LDHs Nanosheets-Coupled V<sub>2</sub>C MXene-Based Heterocatalyst for Enhanced Overall Water Splitting

Deepanshu Malhotra\*, Duy Thanh Tran\*, Nam Hoon Kim\*<sup>†</sup>, Joong Hee Lee\*<sup>\*,\*\*†</sup>

**ABSTRACT:** The rapid increase in the demand for energy has put huge pressure on fossil fuels. The continuous over-utilization of these existing non-renewable energy sources has been causing severe environmental concerns. In these regards, electrochemical water splitting has gained huge attention for producing green hydrogen, a superior energy source with high gravimetric energy density (120 MJ/kg), as compared with conventional options. Electrochemical water splitting is a viable option for generating green hydrogen. However, the various limitations of state-of the art Pt/C and RuO<sub>2</sub>- based electrocatalysts has motivated the scientific community to develop novel cathode (hydrogen evolution reaction (HER)) and anode (oxygen evolution reaction (OER)) electrocatalysts. In our present study, we have achieved a new milestone by fabricating the NiMo-based transition metal LDHs coupled V<sub>2</sub>C MXene support based heterocatalyst. The synergistic impact of NiMo LDHs (corrosion resistance, favorable intrinsic catalytic properties, etc.) and V<sub>2</sub>C (high electrical conductivity, pseudocapacitive behavior, etc.) has resulted in the HER and OER at smaller overpotential of 135 and 370 mV at the current density of 10 and 30 mA cm<sup>-2</sup> in an alkaline (1.0 M KOH) environment.

**Key Words:** NiMo LDHs, V<sub>2</sub>C MXene, HER, and OER, Water splitting

## 1. INTRODUCTION

The demand for energy is increasing proportionally with that of the climbing global population. Existing sources of energy are fossil fuels such as coal, natural gas, etc. However, the surge in energy consumption has put those non-renewable fossil fuels on the verge of exhaustion. In modern-day, these non-renewable fossil fuels have been replaced with renewable forms such as, solar, wind, etc. for energy storage and conversion, but these renewable resources are intermittently delivering energy and thus, couldn't meet the existing industrial energy demands. To address those issues, a zero carbon-emission hydrogen with superior gravimetric energy density is regarded as an ideal candidate to replace contemporary fossil fuels [1]. To produce hydrogen, electrolysis of water is a promising approach. In here, we have HER and OER reactions occurring at cathode and anode, respectively. Owing to the sluggish reaction kinetics, both HER and OER are hampered

by higher overpotential to reach desirable current density. Furthermore, the expensiveness and scarcity of the state-of the art electrocatalysts i.e., Pt- based (HER) and Ru-based oxides (OER) impedes their global usage [2]. Therefore, synthesis of electrocatalysts is of great significance and has gained huge attention from the research community. In the pursuit of electrocatalysts, Ni-based layered double hydroxides (LDHs) materials, has gained highlight because of its superior conductivity, rich surface oxidation states, inexpensiveness alongside favorable OER performance [3,4]. Ni-Mo LDHs is a prominent choice owing to its higher intrinsic catalytic behavior, corrosion resistance in alkaline electrolyte and intermediate binding energy to hydrogen molecule. Despite such properties, these LDHs based material undergoes aggregation due to the electrostatic force within interlayers. This eventually limits the specific surface area and the number of active sites available for electrolysis [5]. Nowadays, a multitude of researchers are exploring various approaches to overcome this setback. In

Received 1 June 2024, received in revised form 18 June 2024, accepted 29 June 2024

\*Department of Nano Convergence Engineering, Jeonbuk National University, Jeonju 54896, Korea

\*\*Carbon Composite Research Center, Department of Polymer-Nano Science and Technology, Jeonbuk National University, Jeonju 54896, Korea

<sup>†</sup>Corresponding authors, Prof. Nam Hoon Kim (E-mail: [nhk@jbnu.ac.kr](mailto:nhk@jbnu.ac.kr)) and Prof. Joong Hee Lee (E-mail: [jhl@jbnu.ac.kr](mailto:jhl@jbnu.ac.kr))

this regard, MXene based catalyst support material has attracted the scientific community. There are various studies that has taken advantages of MXene for enhancing the overall water splitting performance for their respective catalytic system. MXene has various physiochemical characteristics such as, higher electrical conductivity, huge surface area, stability, and hydrophilicity. MXene offers superior redox activity as compared with other carbon-based support and prevent the aggregation of catalyst from previous reports [6,7]. Among various members of the MXene family, V<sub>2</sub>C has been an ideal choice because of its various oxidation states, superior electrical conductivity, and various surface terminations groups. These oxidation states depict the pseudocapacitive behavior which regulates the charge transfer from/to adsorbate and the V<sub>2</sub>C support material [8].

In the present work, we have successfully fabricated the NiMo-LDHs based catalyst supported over V<sub>2</sub>C MXene through a simple solvothermal process. The as-developed electrocatalyst V<sub>2</sub>C-NiMo LDHs delivers favorable HER and OER performances in an alkaline environment (1.0 M KOH) at 25°C with an overpotential of 135 and 370 mV, respectively, at a current density of 10 and 30 mA cm<sup>-2</sup>. Our work could be a potential steppingstone for the synthesis of MXene-based next-generation electrocatalysts for energy conversion applications.

## 2. MATERIALS AND EXPERIMENTAL

### 2.1 Materials

All the chemicals are of analytical grade and used as received without further purification. V<sub>2</sub>AlC MAX phase – 400 mesh was purchased from China (Laizhou Kai Kai Ceramic Materials Co. Ltd.). Hydrofluoric acid (HF, purity 48% (etchant that offers MXene with the coordination of surface terminal group such as: -F), tetrabutylammonium hydroxide solution (TBAOH) ((CH<sub>3</sub>CH<sub>2</sub>CH<sub>2</sub>CH<sub>2</sub>)<sub>4</sub>N(OH), purity 54.0-56.0% in H<sub>2</sub>O) (it's a intercalant agent that increases the interlayer distance of resultant multilayered MXene), nickel (II) nitrate hexahydrate (Ni(NO<sub>3</sub>)<sub>2</sub>·6H<sub>2</sub>O, purity 99.9%) (precursor to synthesis Ni based catalysts), ammonium molybdate tetrahydrate ((NH<sub>4</sub>)<sub>6</sub>Mo<sub>7</sub>O<sub>24</sub>·4H<sub>2</sub>O, purity 81.0-83.0%)(precursor to synthesis Mo based catalysts), urea (CO(NH<sub>2</sub>)<sub>2</sub>, purity ≥ 99.0%) (hydrolysis agent), and sodium citrate tribasic dihydrate (HOC(COONa)(CH<sub>2</sub>COONa)<sub>2</sub>·2H<sub>2</sub>O, purity ≥ 99.0%) (chelating agent) were provided from sigma-Aldrich Chemicals Co. Ltd. (Germany). Potassium hydroxide pellets (KOH, purity 85%), ethanol (C<sub>2</sub>H<sub>5</sub>OH, purity 99%), hydrochloric acid (HCl, purity 37.5 wt.%), were purchased from Samchun Co. (Korea). Nickel foam was provided by Suzhou Yilongsheng Energy Technology Co. Ltd. (China). The Nickel foam was treated under 3.0 M HCl and then washed in ethanol and DI water.

### 2.2 Preparation of exfoliated V<sub>2</sub>C MXene nanosheets

Initially, V<sub>2</sub>AlC powder (1.0 g) was added at slower rate into 20 mL HF (48%) and then transferred to pre heated oil bath at 40°C for 48 h. In the next step, the dark suspension was subjected to washing with deionized (DI) water via centrifugation until the pH reached ~7. The precipitate was then collected after freeze-drying. V<sub>2</sub>AlC etching powder as collected was re-dispersed in 10 mL TBAOH solution and was stirred at room temperature for the next 24 h. The following day, the supernatant was washed multiple times to remove the remaining TBAOH traces. The precipitate was collected and then transferred to 200 mL DI water in a reagent bottle and then was subjected to ultrasonication ice bath for an hour. Finally, the a few-layer delaminated V<sub>2</sub>C MXene was collected with centrifugation (at a run duration and speed for 30 min and 3500 rpm, respectively) using benchtop Allegra X-30 centrifuge, Beckman Coulter and then subjected to further freeze drying.

### 2.3 Synthesis of V<sub>2</sub>C-NiMo LDHs

The V<sub>2</sub>C MXene (30 mg) was added into 50 mL of DI water and then sonicated in an ice bath for an hour. In the next step, Ni(NO<sub>3</sub>)<sub>2</sub>·6H<sub>2</sub>O (1.0 mmole), (NH<sub>4</sub>)<sub>6</sub>Mo<sub>7</sub>O<sub>24</sub>·4H<sub>2</sub>O (0.14 mmole), CO(NH<sub>2</sub>)<sub>2</sub> (3.0 mmole) and HOC(COONa)(CH<sub>2</sub>COONa)<sub>2</sub>·2H<sub>2</sub>O (0.3 mmole) were added to the above MXene dispersion under magnetic stirring at room temperature. After stirring for 15 min, the as-prepared solution was transferred to an oil bath preheated at 90°C for 12 h, the temperature was well-maintained on DAIHAN digital control stirrer (MSH-20D) provided along with temperature probe (SS220). The V<sub>2</sub>C-NiMo LDHs material was collected after centrifugation at 4000 rpm for 10 min. The V<sub>2</sub>C-NiMo LDHs were dried for at least 3 days using iLshinoBioBase Freeze Dryer machine, maintain at -85°C condenser temperature along with vacuum pressure (< 10 mTorr).

### 2.4 Material characterizations

To characterize the surface structure of the as-fabricated samples, field-emission scanning electron microscopy, Carl Zeiss, Supra 40 VP, Germany was utilized. The powder XRD patterns were investigated via D/MAX 2500 V/PC, Rigaku provided with a Cu K $\alpha$  radiation (40 kV,  $\lambda$  = 0.154 nm and 40 mA).

### 2.5 Electrochemical characterizations

The electrochemical performance for the as-prepared samples was analyzed using a CHI660D workstation. Linear sweep voltammetry for as-prepared samples was characterized using a 3-electrode system in 1.0 M KOH electrolyte at a sweep scan rate of 5 mV s<sup>-1</sup> and iR-compensation (100%) was used for correction. The iR compensation was performed to compensate the voltage difference caused due to alkaline electrolyte in between the working electrode and the reference electrode (Ag/AgCl), the calculations are based on the equation:  $E_{iR-compen}$

$= E_{\text{meas}} - I_{\text{meas}} \times R_c$ , where  $R_c$ ,  $E_{iR\text{-compensated}}$ ,  $E_{\text{meas}}$ ,  $I_{\text{meas}}$  represents compensated resistance,  $iR$ -compensated potential, measured potential and measured current. Herein, the Nickel foam (1 cm  $\times$  1 cm) acted as a working electrode. To prepare the working electrode, 750  $\mu\text{L}$  IPA containing 20  $\mu\text{L}$  Nafion and 2.5 mg of catalyst was sonicated in an ice bath for an hour. Later, the resultant ink was drop-casted on nickel foam (1 cm  $\times$  1 cm) and dried prior to use at ambient room temperature. Ag/AgCl and graphite electrode were used as reference and counter electrode, respectively.

### 3. RESULTS AND DISCUSSION

#### 3.1 $\text{V}_2\text{C}$ -NiMo LDHs synthesis and morphology characterizations

The synthesis of  $\text{V}_2\text{C}$ -NiMo LDHs hybrid nanoarchitecture can be achieved via a facile co-precipitation approach, as clearly illustrated stepwise in Scheme 1. Initially, the multi layered  $\text{V}_2\text{C}$  MXene nanosheet was used as a stiff support owing to its superior electrical conductivity along with the favorable mechanical properties and is synthesized through etching of aluminum layers from the structure of  $\text{V}_2\text{AlC}$  max powder by using HF solution (48%), followed with the few-layered  $\text{V}_2\text{C}$  MXene with functionalized surface is obtained after treatment with TBAOH and exfoliation under ice bath sonication. This renders the  $\text{V}_2\text{C}$  Mxene with surface terminal group that assist in nucleation and growth of LDHs. In further steps, the  $\text{V}_2\text{C}$ -NiMo LDHs hybrid nanostructure is achieved by introducing  $\text{Ni}^{2+}$  and  $\text{Mo}^{6+}$  metal precursors to  $\text{V}_2\text{C}$  MXene dispersion. The synergistic impact of flexible shell (NiMo LDHs) and the stiff support ( $\text{V}_2\text{C}$  Mxene), offers rapid electron transfer between the LDHs and  $\text{V}_2\text{C}$  support that as a result lowers the overpotential for the HER and OER activity.

Scanning electron microscopy (SEM) analysis data for the as-developed  $\text{V}_2\text{C}$  MXene material confirms the successful exfoliation into few-layers  $\text{V}_2\text{C}$  Mxene (Fig. 1A and B).

As shown in (Fig. 1C and D), the  $\text{V}_2\text{C}$  MXene is covered with 2D nanosheets of NiMo LDHs, that resembles honeycomb-like morphology. Furthermore, the distributions for V, C, O, Ni, and Mo over a surveyed region are indicated in the respective elemental-mapping, confirming the synthesis of

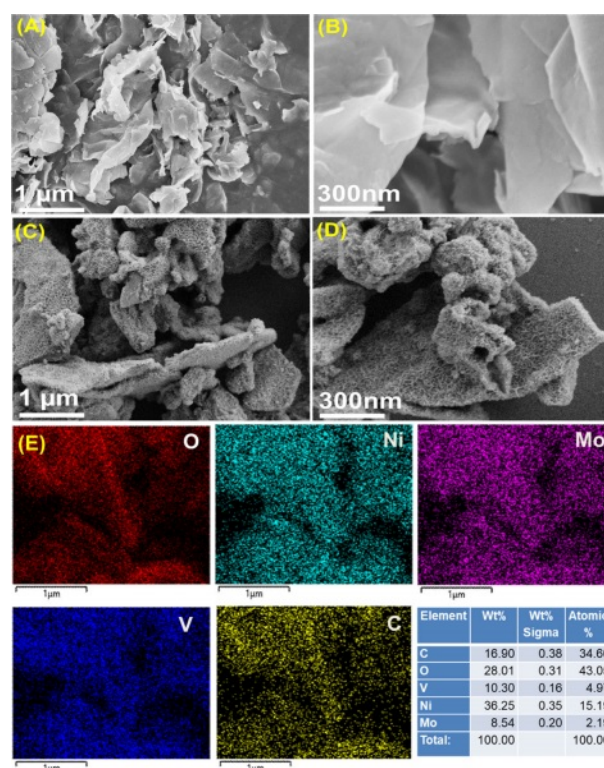


Fig. 1. SEM images of (A, B)  $\text{V}_2\text{C}$  MXene and (C,D)  $\text{V}_2\text{C}$ -NiMo LDHs; (E) Corresponding EDS spectrum of the  $\text{V}_2\text{C}$ -NiMo LDHs

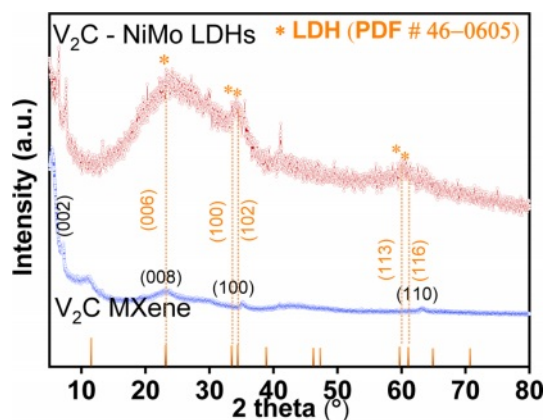
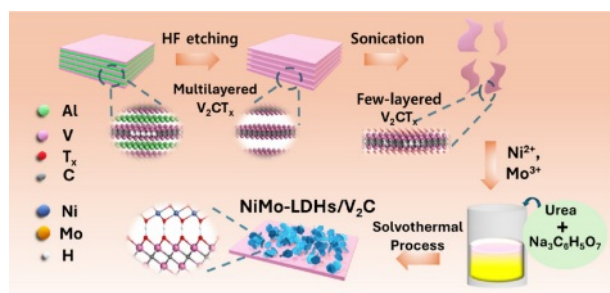


Fig. 2. XRD patterns of  $\text{V}_2\text{C}$ -NiMo LDHs and  $\text{V}_2\text{C}$  MXene materials



Scheme 1. Schematic representation of the synthesis for  $\text{V}_2\text{C}$ -NiMo-LDHs electrocatalyst

NiMo LDHs nanosheets anchored on  $\text{V}_2\text{C}$  MXene (Fig. 1E).

To examine the crystalline properties of the  $\text{V}_2\text{C}$ -NiMo LDHs and  $\text{V}_2\text{C}$  MXene, X-ray diffraction (XRD) technique was applied, as represented from (Fig. 2). The  $2\theta$  corresponding to  $7.3^\circ$  is a characteristic of the (002) crystal plane. Moreover, the presence of minor peaks corresponds to  $\text{V}_2\text{AlC}$  in the  $\text{V}_2\text{C}$  material's diffraction pattern could result from the unreacted MAX phase in the final product [9,10]. The diffraction peaks located at  $2\theta$  of  $23.2^\circ$ ,  $33.6^\circ$ ,  $34.5^\circ$ , and  $59.9^\circ$  and  $61.2^\circ$  in  $\text{V}_2\text{C}$ -NiMo LDHs material represent the corresponding planes

of (006), (100), (102), (113), and (116) in LDHs (# PDF 46-0605). The broadening of the peak at around 23.2° could be impact of synergistic effect of crystalline nature of Ni and Mo and their bonding, as indicated in previous published literature [11].

### 3.2 Electrochemical evaluation of the V<sub>2</sub>C-NiMo LDHs

HER performance for the as-synthesized samples was analyzed under room temperature in 1.0 M KOH using the LSV technique at a sweep rate of 5 mV s<sup>-1</sup>. The observations have indicated that among various catalysts, V<sub>2</sub>C-NiMo LDHs have shown significantly superior performance along with the lower overpotential  $\eta$  of 135 mV at the current density of 10 mA cm<sup>-2</sup> (Fig. 3A). To illustrate the reaction kinetics for the various surveyed catalysts, we have investigated the Tafel slopes (Fig. 3B). The V<sub>2</sub>C@NiMo LDHs sample has smallest Tafel value (128.3 mV dec<sup>-1</sup>), as compared with V<sub>2</sub>C MXene (143.2 mV dec<sup>-1</sup>), indicating that V<sub>2</sub>C@NiMo LDHs operates at rapid rate and the as-fabricated electrocatalyst follows Volmer-Heyrovsky mechanism. Herein, HER in an alkaline medium is well-controlled with the Volmer reaction (the generation of adsorbed hydrogen) and the Heyrovsky mechanism (a crucial step that regulates the combination of the water molecule with that of adsorbed hydrogen to produce a hydrogen

molecule.) [12]. This result indicates that the combination of MXene nanosheets and NiMo LDHs can produce specific synergistic effects to promote the number of electroactive sites and charge conductivity, thus leading to the enhanced hydrogen production possibility via the HER process.

To investigate the bifunctional performance of the developed catalyst, the OER activity of the V<sub>2</sub>C, V<sub>2</sub>C-NiMo LDHs, and commercial RuO<sub>2</sub> was studied in 1.0 M KOH medium. The OER performance for the given catalysts was studied via LSV at a sweep rate of 5.0 mV s<sup>-1</sup>. The results conclude that the V<sub>2</sub>C-NiMo LDHs have superior performance towards OER at a lower overpotential  $\eta$  of 370 mV, in comparison to V<sub>2</sub>C MXene (530 mV) @ 30 mA cm<sup>-2</sup> (Fig. 4A). To understand the reaction kinetics, we derived the Tafel plot from the iR-compensated LSV results, as shown in (Fig. 4B). The Tafel plot comparison for the given materials were in the order of V<sub>2</sub>C-NiMo LDHs (179.9 mV dec<sup>-1</sup>) < RuO<sub>2</sub> (210.5 mV dec<sup>-1</sup>) < pure V<sub>2</sub>C MXene (307.2 mV dec<sup>-1</sup>). The as-developed V<sub>2</sub>C-NiMo LDHs favor the faster reaction mechanism towards oxygen evolution at the anode. The achieved results of the V<sub>2</sub>C-NiMo LDHs materials towards OER indicate that the hybridization of NiMo LDHs over the surface of V<sub>2</sub>C MXene structure results in the change of electronic properties and charge reconfiguration of electroactive sites to be higher valence states for

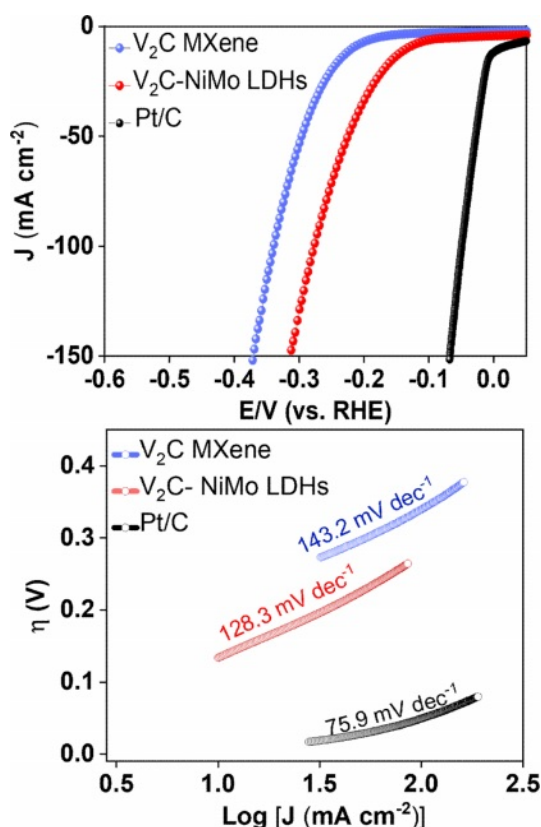


**Fig. 3.** (A) iR-compensated LSV plot and (B) Tafel slopes of the various as-synthesized electrocatalysts for alkaline HER process in alkaline medium

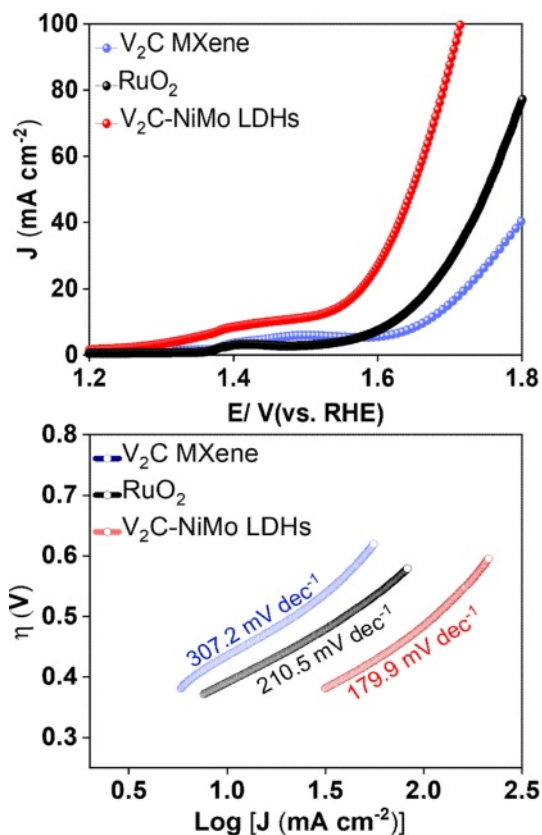


**Fig. 4.** (A) iR-compensated LSV plot and (B) Tafel slopes of the various as-synthesized electrocatalysts for alkaline OER process in alkaline medium

effectively facilitating the OER activity.

#### 4. CONCLUSIONS

In this study, we have successfully fabricated the  $V_2C$ -NiMo LDHs nanosheets based heterostructure. This unique composite architecture promotes the synergistic effect of MXene-based support and the honeycomb-based shell via enhancement of physiochemical properties for the given electrocatalyst such as improved active sites, and superior conductivity, thus, offering powerful HER and OER performances in an alkaline condition with lower overpotential of 135 mV and 370 mV at the current density of 10 and 30 mA cm<sup>-2</sup>. These results could form an interesting basis for improvising further electrode materials toward high-efficiency hydrogen generation via electrochemical water splitting.

#### REFERENCES

1. Nguyen, T.H., Tran, P.K.L., Dinh, V.A., Tran, D.T., Kim, N.H., and Lee, J.H., "Metal Single-Site Molecular Complex-Mxene Heteroelectrocatalysts Interspersed Graphene Nanonetwork for Efficient Dual-Task of Water Splitting and Metal-Air Batteries," *Advanced Functional Materials*, Vol. 33, No. 7, 2023, 2210101.
2. Malhotra, D., Nguyen, T.H., Tran, D.T., Dinh, V.A., Kim, N.H., and Lee, J.H., "Triphasic Ni<sub>2</sub>P-Ni<sub>12</sub>P<sub>5</sub>-Ru with Amorphous Interface Engineering Promoted by Co Nano-Surface for Efficient Water Splitting," *Small*, Vol. 20, 2024, 2309122.
3. Bao, J., Wang, Z., Xie, J., Xu, L., Lei, F., Guan, M., Huang, Y., Zhao, Y., Xia, J., and Li, H., "The CoMo-LDH Ultrathin Nanosheet As a Highly Active and Bifunctional Electrocatalyst for Overall Water Splitting," *Inorganic Chemistry Frontiers*, Vol. 5, 2018, pp. 2964-2970.
4. Yang, L., Liu, Z., Zhu, S., Feng, L., and Xing, W., "Ni-based Layered Double Hydroxide Catalysts for Oxygen Evolution Reaction," *Materials Today Physics*, Vol. 16, 2021, 100292.
5. Boumeriame, H., Da Silva, E.S., Cherevan, A.S., Chafik, T., Faria, J.L., and Eder, D., "Layered Double Hydroxide (LDH)-based Materials: A Mini-Review on Strategies to Improve the Performance for Photocatalytic Water Splitting," *Journal of Energy Chemistry*, Vol. 64, 2021, pp. 406-431.
6. Lv, Z., Ma, W., Dang, J., Wang, M., Jian, K., Liu, D., and Huang, D., "Induction of Co<sub>2</sub>P Growth on a MXene (Ti<sub>3</sub>C<sub>2</sub>T<sub>x</sub>)-Modified Self-Supporting Electrode for Efficient Overall Water Splitting," *The Journal of Physical Chemistry Letters*, Vol. 12, No. 20, 2021, pp. 4841-4848.
7. Selvam, N.C.S., Lee, J., Choi, G.H., Oh, M.J., Xu, S., Lim, B., and Yoo, P.J., "MXene Supported CoxAy (A = OH, P, Se) Electrocatalysts for Overall Water Splitting: Unveiling the Role of Anions in Intrinsic Activity and Stability," *Journal of Materials Chemistry A*, No. 7, 2019, pp. 27383-27393.
8. Chen, Y., Yao, H., Kong, F., Tian, H., Meng, G., Wang, S., Mao, X., Cui, X., Hou, X., and Shi, J., "V<sub>2</sub>C MXene Synergistically Coupling FeNi LDH Nanosheets for Boosting Oxygen Evolution Reaction," *Applied Catalysis B: Environment and Energy*, Vol. 297, 2021, 120474.
9. Nguyen, T.H., Tran, P.K.L., Tran, D.T., Dinh, V.A., Kim, N.H., and Lee, J.H., "Ru-Ru<sub>2</sub>P Hetero-Cluster Promoted V<sub>2</sub>CT<sub>x</sub> Sheets-Based Electrocatalyst Enables Industrial-Level AEM Water Electrolysis," *Applied Catalysis B: Environment and Energy*, Vol. 343, 2024, 123517.
10. Deng, Q., Chen, B., Bo, M., Feng, Y., Huang, Y., and Zhou, J., "Interfacial Fluorine Migration-Induced Low Leakage Conduction in PVA Based High-k Composites with V<sub>2</sub>C MXene-SWCNT Switchboard-Like Ceramic Via ab initio MD Simulations," *Journal of Materials Chemistry C*, Vol. 9, No. 3, 2021, pp. 1051-1061.
11. Shen, W.C., Hu, T.T., Liu, X.Y., Zha, J.J., Meng, F.Q., Wu, Z.K., Cui, Z.L., Yang, Y., Li, H., Zhang, Q.H., Gu, L., Liang, R.Z., and Tan, C.L., "Defect Engineering of Layered Double Hydroxide Nanosheets As Inorganic Photosensitizers For NIR-III Photodynamic Cancer Therapy," *Nature Communications*, Vol. 13, 2022, p. 3384.
12. Tran, P.K.L., Tran, D.T., Austeria P.M., Kim, D.H., Kim, N.H., and Lee, J.H., "Intermolecular Metallic Single-Site Complexes Dispersed on Mo<sub>2</sub>TiC<sub>2</sub>T<sub>x</sub>/MoS<sub>2</sub> Heterostructure Induce Boosted Solar-Driven Water Splitting," *Advanced Energy Materials*, Vol. 13, No. 15, 2023, 2203844.